Article ID: 1007-4627(2024) 03-0001-07

CNPC2023 Exploring the feasibility of producing superheavy nuclei in the proton evaporation channel

Lu-Qi Li[1], Gen Zhang[1], Jun-Jun Cai[1], Li-Lin Zhou[1], Feng-Shou Zhang[2, 3, 4]

(*1. School of Physical Science and Technology, Guangxi University, Nanning 530004, China;*
2. College of Nuclear Science and Technology, Beijing Normal University, Beijing 100875, China;
3. Beijing Radiation Center, Beijing 100875, China;
4. Center of Theoretical Nuclear Physics, National Laboratory of Heavy Ion Accelerator of Lanzhou, Lanzhou 730000, China)

Abstract: The feasibility of producing superheavy nuclei in proton evaporation channels was systematically studied within the dinuclear system (DNS) model. Due to the Z=114 proton-shell, one can synthesize Fl isotopes in proton evaporation channels. We only considered the case of evaporating one proton first and then n neutrons in this work, other cases were ignored due to the small cross-section. The production cross sections of unknown isotopes ^{290,291}Fl in ^{38}S+^{255}Es reaction are the highest compared with ^{50}Ti+^{243}Np and ^{54}Cr+^{239}Pa reactions, and the maximum cross sections are 1.1 and 15.1 pb, respectively. ^{42}S+^{254}Es is a promising candidate to approach the island of stability as the radioactive beam facilities are upgraded in the future, and the production cross sections of $^{291-294}$Fl in that reaction are estimated to be 3.2, 6.0, 4.0, and 0.1 pb, respectively.

Key words: DNS model; superheavy nuclei; fusion reaction; proton evaporation channel; production cross section
CLC number: O571.42 **Document code:** A **DOI:** 10.11804/NuclPhysRev.37.01.01

Introduction

The synthesis of superheavy nuclei has always been an important task and challenge in nuclear physics, which is significant to expand the nuclear map, investigate the origin of heavy elements, and test the shell model. At present, the research on the synthesis of superheavy nuclei can be divided into two directions. One is to synthesize new elements to explore the charge limit of superheavy nuclei [1-3]. The other is to move towards to the double magic nuclei ^{298}Fl, which is the center of the island of stability[4-7]. Because the β stability line bends towards the neutron axis, the currently produced superheavy nuclei based on fusion-evaporation reactions are neutron-deficient, and very far away from the island of stability. That requires us to strive towards the development of radioactive beam facilities and the search for new production mechanisms.

Several models have been developed to study the fusion mechanism and predict the production cross-sections of superheavy nuclei. The semi-classical models, such as the multidimensional Langevin-type dynamical equations[8], the nuclear collectivization model[9], the fusion-by-diffusion model[10] and the dinuclear system model[11-13], have been successfully applied to calculate the evaporation-residue (ER) cross sections of superheavy nuclei. The microscopic models like TDHF approach[14-15] and ImQMD model[16-17] can effectively describe the dynamical dissipation during the fusion process.

In this work, we attempted to produce superheavy nuclei in proton evaporation channels. To this end, we have developed the de-excitation part in the DNS model and found the production of Fl isotopes in proton evaporation channels is considerable.

1 The DNS model

Within the framework of DNS, the ER cross sections of superheavy nuclei at the incident energy $E_{\rm c.m.}$ are calculated

Received date: 26 Jan. 2024; **Revised date:** 26 Jan. 2024
Foundation item: Guangxi Natural Science Foundation (2022GXNSFBA035549)
Biography: Lu-Qi Li(1997–), Zibo, Shandong Province, Postgraduate, Working on nuclear physics; E-mail: liluqi@st.gxu.edu.cn

by [18]:

$$\sigma_{\rm ER}(E_{\rm c.m.}) = \frac{\pi\hbar^2}{2\mu E_{\rm c.m.}}\sum_{J=0}^{J_{\max}}(2J+1)T(E_{\rm c.m.},J) \times P_{\rm CN}(E_{\rm c.m.},J)W_{\rm sur}(E_{\rm c.m.},J). \quad (1)$$

Here, T, $P_{\rm CN}$, and $W_{\rm sur}$ are the transmission, fusion, and survival probability, respectively.

It is difficult to obtain an analytical expression for the transmission probability due to the complexity of the actual Coulomb barrier, and it can be obtained by using the WKB method after making a parabolic approximation of the Coulomb barrier[19]:

$$T(E_{\rm c.m.},J) = \int f(B) \frac{1}{1+\exp\{-\frac{2\pi}{\hbar\omega(J)}[E_{\rm c.m.}-B-\frac{\hbar^2}{2\mu R_B^2(J)}J(J+1)]\}}dB. \quad (2)$$

Here, $\hbar\omega$ is the width of the parabolic barrier and R_B defines the position of the barrier. Considering the multi-dimensional character of the realistic barrier, the barrier distribution function $f(B)$ should be introduced, which is taken as the asymmetric Gaussian form[9].

The interaction potential after considering deformation can be written as

$$V(R,\beta_1,\beta_2,\theta_1,\theta_2) = V_C(R,\beta_1,\beta_2,\theta_1,\theta_2) + V_N(R,\beta_1,\beta_2,\theta_1,\theta_2) + \frac{1}{2}C_1(\beta_1-\beta_1^0)^2 + \frac{1}{2}C_2(\beta_2-\beta_2^0)^2, \quad (3)$$

where V_C and V_N are Coulomb potential and nuclear potential, given by Wong's formula and double folding method, respectively. $\beta_{1,2}^0$ is the static deformation (for nuclei 1 and 2), usually taken as the quadrupole deformation. $\beta_{1,2}$ is the dynamical deformation. Assuming that the deformation energy is proportional to the mass number, i.e. $C_1\beta_1^2/C_2\beta_2^2 = A_1/A_2$, only one deformation parameter $\beta = \beta_1 + \beta_2$ can be used to represent the dynamical deformation. $C_{1,2}$ are the coefficients that characterize nuclear hardness and given by

$$C = (\lambda-1)\left[(\lambda+2)R_N^2\sigma - \frac{3}{2\pi}\frac{Z^2e^2}{R_N(2\lambda+1)}\right]. \quad (4)$$

Here, R_N is the nuclear radius, λ is the deformation number, taking 2 for quadrupole deformation. σ is the surface tension coefficient and given by $4\pi R^2\sigma = a_s A^{2/3}$, where a_s is taken as 18.32 MeV.

The distribution probability $P(Z_1,N_1,t)$ for the fragment (Z_1,N_1) at time t is determined by solving the master equation[20]:

$$\frac{dP(Z_1,N_1,t)}{dt} = \sum_{Z_1'}W_{Z_1,N_1;Z_1',N_1}(t)[d_{Z_1,N_1}P(Z_1',N_1,t) - d_{Z_1',N_1}P(Z_1,N_1,t)] + \sum_{N_1'}W_{Z_1,N_1;Z_1,N_1'}(t)[d_{Z_1,N_1}P(Z_1,N_1',t) - d_{Z_1,N_1'}P(Z_1,N_1,t)] - [\Lambda_{\rm qf}(\Theta(t)) + \Lambda_{\rm fis}(\Theta(t))]P(Z_1,N_1,t) \quad (5)$$

Here, d_{Z_1,N_1} discribes the microscopic dimension corresponding to the macroscopic state (Z_1,N_1). $\Lambda_{\rm qf}$ and $\Lambda_{\rm fis}$ are the quasifission and fission rates, calculated by the one-dimensional Kramers equation[21]. $\Theta(t) = \sqrt{\varepsilon^*/a}$ is the local temperature, obtained from the Fermi gas model, where ε^* is the local excitation energy of the dinuclear system, and a is the level density parameter. $W_{Z_1,N_1;Z_1',N_1}(W_{Z_1,N_1;Z_1,N_1'})$ is the transition probability from state (Z_1,N_1) to (Z_1',N_1) (or from (Z_1,N_1) to (Z_1,N_1')), which can be written as:

$$W_{Z_1,N_1;Z_1',N_1}(t) = \frac{\tau_{\rm mem}(Z_1,N_1,E_1,Z_1',N_1,E_1';t)}{\hbar^2 d_{Z_1,N_1}d_{Z_1',N_1}} \times \sum_{ii'}|<Z_1',N_1,E_1',i'|V(t)|Z_1,N_1,E_1,i>|^2. \quad (6)$$

Here, i represents the remaining quantum numbers. E_1 denotes the local excitation energy. $\tau_{\rm mem}$ is the memory time and given by[22]

$$\tau_{\rm mem}(A_1,E_1,A_1',E_1',t) = \hbar\sqrt{\frac{2\pi}{\sum_{KK'}<V_{KK'}V_{KK'}^*>}}. \quad (7)$$

The compound nucleus formed by fusion reaction has high excitation energy and deexcites by emission of γ-rays, light particles and fission. According to Weisskopf's evaporation theory[23], the evaporation width of particle ν can be written as:

$$\Gamma_\nu(E^*,J) = (2s_\nu+1)\frac{m_\nu}{\pi^2\hbar^2\rho(E^*,J)} \times\int_0^{E^*-B_\nu-\delta-\delta_n-\frac{1}{a}}\varepsilon\rho(E^*-B_\nu-\delta_n-\varepsilon)\sigma_{\rm inv}(\varepsilon)d\varepsilon, \quad (8)$$

where B_ν, m_ν, and s_ν are the binding energy, mass, and spin of the particle, respectively. The pairing correction δ is set to be $12/\sqrt{A}$, 0, and $-12/\sqrt{A}$ for even-even, odd-A, and odd-odd nuclei, respectively. δ_n is the neutron correction energy.

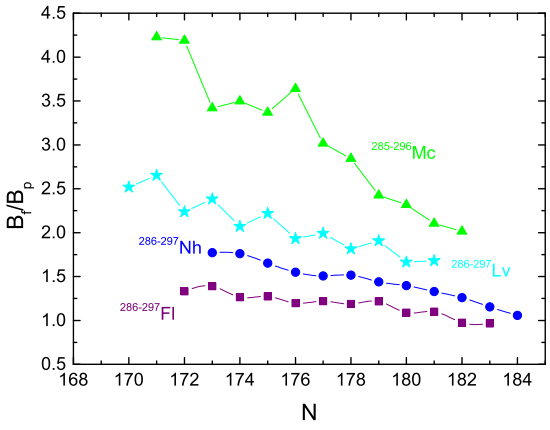

Fig. 1 (color online) The ratios B_f/B_p of nuclei $^{286-297}$Nh, $^{286-297}$Fl, $^{285-296}$Mc, and $^{286-297}$Lv are denoted by the circles, squares, triangles, and pentagrams, respectively.

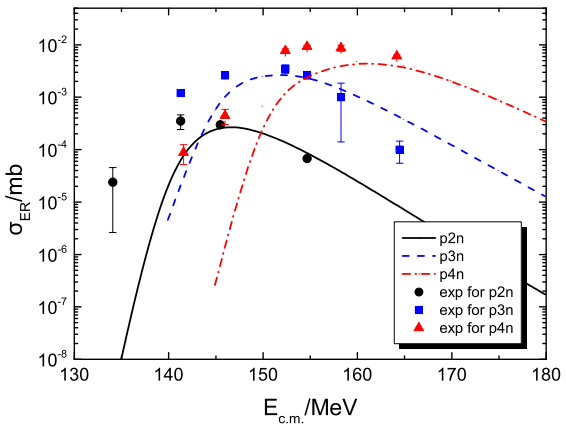

Fig. 2 (color online) Comparisons of calculated evaporation residual cross sections with the experimental data in ^{40}Ar+^{179}Hf reactions. The solid, dashed, and dash-dotted lines represent the calculated evaporation residual cross sections in *p2n*, *p3n*, and *p4n* evaporation channels respectively. The circles, squares, and triangles represent the experimental data with error bars in *p2n*, *p3n*, and *p4n* evaporation channels, respectively. The experimental data are obtained from Ref.[25]

If the neutron number of the compound nucleus is odd, $\delta_n = 12/\sqrt{A}$, and δ_n =0 in other cases. ρ is the energy level density and calculated by the Fermi-gas model. The level density parameter a is given by

$$a(E^*, Z, N) = \tilde{a}(A)[1 + E_{sh}(Z, N)f(E^* - \Delta)/(E^* - \Delta)] \quad (9)$$

Here, asymptotic Fermi-gas value of the level density parameter $\tilde{a}(A) = \alpha A + \beta A^{2/3} b_s$. $E_{sh}(Z, N)$ is the shell correction energy, and $f(E^*)$ is the shell damping factor. The parameters α, β and b_s are taken to be 0.114, 0.098 and 1.0, respectively. The inverse cross section σ_{inv} is given by the following formula :

$$\sigma_{inv}(\varepsilon) = \begin{cases} \pi R_\nu^2(1 - \frac{V_\nu}{\varepsilon}), & \varepsilon > V_\nu \\ 0, & \varepsilon < V_\nu \end{cases} \quad (10)$$

where R_ν can be expressed as:

$$R_\nu = 1.16[(A - A_\nu)^{1/3} + A_\nu^{1/3}]. \quad (11)$$

Here, A_ν is the mass number of the evaporated particle. For proton evaporation, the Coulomb barrier V_ν is parameterized by the following formula :

$$V_\nu = [1.15Z_\nu(Z - Z_\nu)]/(R_\nu + 1.6). \quad (12)$$

The survival probability of a superheavy nucleus can be expressed as[23]:

$$W_{sur}(E^*_{CN}, x, y, J) = P(E^*_{CN}, x, y, J) \times \prod_{i=1}^{x} \frac{\Gamma_p(E_i^*, J)}{\Gamma_{tot}(E_i^*, J)} \prod_{j=x+1}^{x+y} \frac{\Gamma_n(E_j^*, J)}{\Gamma_{tot}(E_j^*, J)}, \quad (13)$$

where $\Gamma_{tot} = \Gamma_n + \Gamma_p + \Gamma_f$. The fission width Γ_f is given by the Bohr Wheeler formula,

$$\Gamma_f(E^*, J) = \frac{1}{2\pi\rho_f(E^*, J)} \int_0^{E^* - b_f - \delta - \frac{1}{a_f}} \frac{\rho_f(E^* - b_f - \varepsilon, J)d\varepsilon}{1 + \exp[-2\pi(E^* - b_f - \varepsilon)/\hbar\omega]}. \quad (14)$$

Here, $P(E^*_{CN}, x, y, J)$ is the realization probability, which is given by the Jackson formula[24]. E_i^* is the excitation energy before evaporating the i-th particle. B_i^ν is the separation energy of the i-th particle. T_i is nuclear temperature before the i-th particle evaporated, obtained from $T_i = \sqrt{E_i^*/a}$.

2 Results and discussion

Firstly, in order to find the compound nuclei with the largest cross section in the proton evaporation channel, we defined a ratio B_f/B_p to evaluate the strength of proton evaporation of the compound nuclei. Fig. 1 shows the calculated ratios B_f/B_p of nuclei $^{286-297}$Nh, $^{286-297}$Fl, $^{285-296}$Mc, and $^{286-297}$Lv which denoted by the circles, squares, triangles, and pentagrams, respectively. It can be seen that the ratios B_f/B_p of $^{285-296}$Mc are the highest and the fission bar-

rier is approximately 2-4 times the proton separation energy, which means that proton evaporation is easier for $^{285-296}$Mc during the de-excitation process, resulting in a larger proton evaporation probability. The ratios B_f/B_p of $^{286-297}$Fl are the smallest, which means that $^{286-297}$Fl is hard to evaporate protons due to the proton closed-shell at Z = 114. From that, one can first synthesize compound nuclei with Z=115, and then obtain the Fl isotopes by evaporating one proton and *n* neutrons.

To verify the reliability of the DNS model，we calculated the ER cross sections in ^{40}Ar+^{179}Hf reactions as shown in Fig. 2. The *p*2*n*, *p*3*n*, and *p*4*n* evaporation channels are denoted by solid, dashed, and dash-dotted lines, respectively. The experimental data in *p*2*n*, *p*3*n*, and *p*4*n* evaporation channels are represented by circles, squares, and triangles, respectively[25]. It can be seen that the calculated results are in good agreements with the experimental data, but at low incident energy the calculated results are significantly lower than the experimental data. This is because in the de-excitation process, the evaporation of charged particles is based on classical considerations and the quantum tunneling effect is not consider.

In order to produce superheavy nuclei in proton evaporation channel, firstly it is necessary to consider the number and order of the evaporated protons. Therefore, in Fig. 3, we calculated the evaporation width of ^{48}Ca+^{243}Am reaction in which the Mc compound nuclei can be produced. It can be seen that the proton evaporation width is the smallest.

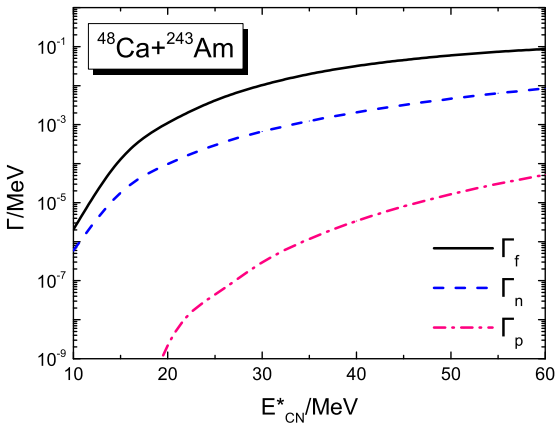

Fig. 3 (color online) The calculated evaporation width of compound nucleus ^{291}Mc produced by ^{48}Ca+^{243}Am reaction. The solid, dashed, and dash-dotted lines represent the widths of fission, neutron, and proton, respectively.

Compared to neutron evaporation width, the survival probability decreases by 1-2 orders of magnitude after each proton evaporated. Therefore, in this work, we only considered the case of evaporating one proton, and the survival probability of multiple protons evaporated is too small, which can be ignored. Secondly, as the excitation energy decreases, the proton evaporation width decreases very quickly, and the ratio Γ_p/Γ_n decreases. The survival probability will be reduced by 1-2 orders of magnitude after each proton evaporated. In the end, we only consider the case where one proton is evaporated firstly and then *n* neutrons are evaporated, and the survival probability in other cases is ignored.

The ER cross sections in ^{38}S+^{255}Es, ^{50}Ti+^{243}Np, ^{54}Cr+^{239}Pa, and ^{42}S+^{254}Es reactions for producing Fl isotopes are shown in Fig. 4. Solid, dashed, dash-dotted, and dotted lines represent *p*1*n*, *p*2*n*, *p*3*n*, and *p*4*n* evaporation channels, respectively. For these reactions, the ER cross sections in *p*2*n* and *p*3*n* channels are relatively larger. One can find that the ER cross sections in the reaction ^{38}S+^{255}Es are the highest among the previous three reactions corresponding to the same compound nucleus. That is because the mass asymmetry for the ^{38}S+^{255}Es reaction is the largest, leading to the highest fusion probability. The maximum ER cross sections of unknown isotopes ^{290,291}Fl are 1.1 pb and 15.1 pb at E^*_{CN} = 38.2 MeV and 39.4 MeV, respectively. ^{38}S beam can be produced by the fragmentation of ^{40}Ar at a projectile fragmentation facility[26], and the fusion reactions ^{38}S + ^{181}Ta and ^{38}S + ^{208}Pb with ^{38}S beam were conducted successfully.

In order to produce more unknown Fl isotopes, the ER cross sections in the radioactive beam induced reaction, ^{42}S+^{254}Es, are also predicted. Four unknown isotopes ,$^{291-294}$Fl, are synthesized with cross sections 3.2, 6.0, 4.0, and 0.1 pb at E^*_{CN} = 42.2, 28.6, 20.2, and 15.0 MeV, respectively. One can notice that the ER cross sections in ^{42}S+^{254}Es reaction in p4n channel are comparable to those in *p*2*n* and *p*3*n* channels unlike the other three reactions. That is because the compound nucleus in the reaction ^{42}S+^{254}Es has more neutrons than the other three reactions, leading to the highest survival probability in *p*4*n* channel. If the radioactive beam facilities are upgraded and the intensity of the ^{42}S beam is increased to a high quantity in the future, the reaction ^{42}S+^{254}Es can be a promising candidate to approach the island of stability.

Considering the sensitivity of the DNS model to certain

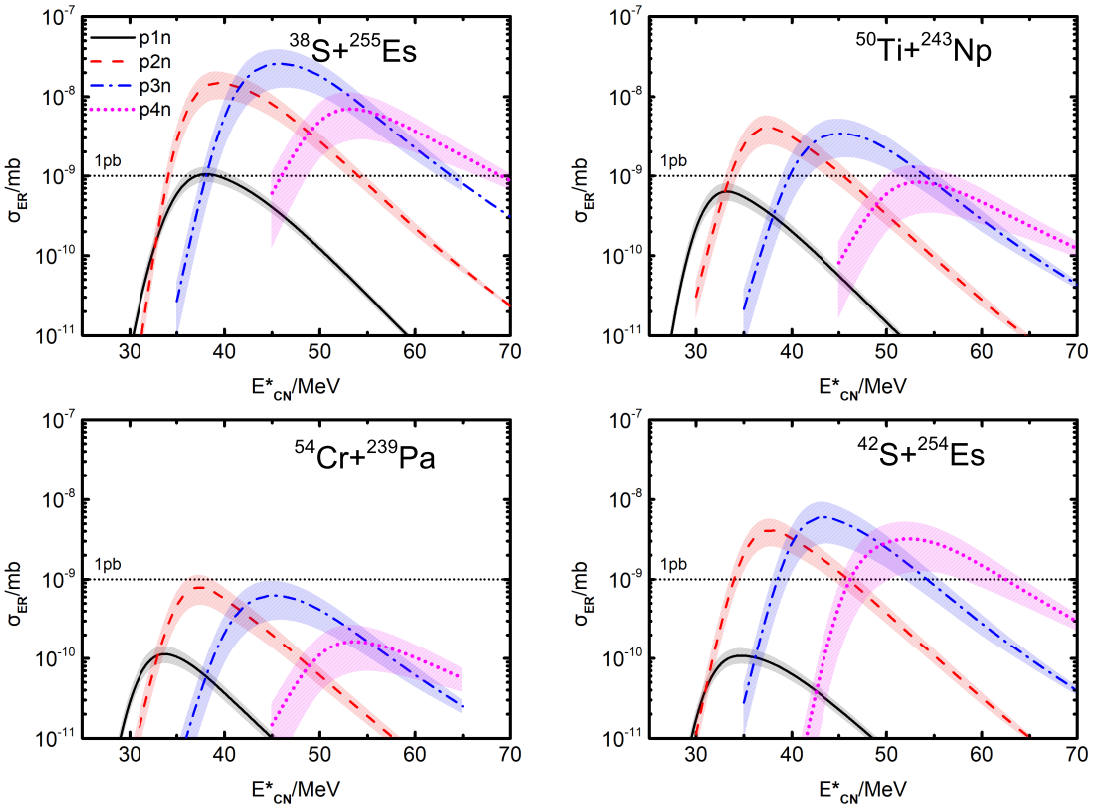

Fig. 4 (color online) The calculated evaporation residual cross sections in ^{38}S+^{255}Es, ^{50}Ti+^{243}Np, ^{54}Cr+^{239}Pa, and ^{42}S+^{254}Es reactions. Solid, dashed, dash-dotted, and dotted lines represent p1n, p2n, p3n, and p4n evaporation channels, respectively. Shadow area represents the calculated error.

parameters, it is necessary to evaluate the inaccuracy of theoretical calculations in order to find out the uncertainty of predictions. Among the parameters in the model, the shell damping factor $E_{\rm d}$ plays a vital role in the ER cross sections[27]. The shell damping factor cannot be precisely determined both experimentally and theoretically, and its inaccuracy is considered based on the experimental data in the Ref.[28]. The uncertainty of the calculation results is shown in the shadow in Fig. 4. It can be seen that the uncertainties of the ER cross sections of Fl isotopes are no better than one order of magnitude, and the uncertainties of the optimal excitation energy are only in the order of 0.1 MeV.

3 Summary

In summary, the production of Fl isotopes in proton evaporation channels is investigated within the DNS model. Among the isotopes around $Z = 114$, proton evaporation is the easiest for Mc isotopes but the most difficult for Fl isotopes due to the proton closed-shell at $Z = 114$. Hence, one can synthesize the Fl isotopes in the proton evaporation channel. The calculated ER cross sections by the DNS model reproduce the experimental data very well. The synthesis of unknown isotopes ^{290,291}Fl is studied via ^{38}S+^{255}Es, ^{50}Ti+^{243}Np, and ^{54}Cr+^{239}Pa reactions corresponding to the same compound nucleus. The ER cross sections of ^{290}Fl and ^{291}Fl in the reaction ^{38}S+^{255}Es are the largest, which are 1.1 pb and 15.1 pb at $E^*_{\rm CN} = 38.2$ MeV and 39.4 MeV, respectively. In the radioactive beam induced reaction ^{42}S+^{254}Es, four new isotopes $^{291-294}$Fl are synthesized with ER cross sections of 3.2, 6.0, 4.0, and 0.1 pb at $E^*_{\rm CN} = 42.2$, 28.6, 20.2, and 15.0 MeV, respectively. The uncertainties of the predictions from the inaccuracy of the shell damping factor are calculated, and the uncertainties of the ER cross sections of Fl isotopes are no better than one order of magnitude.

4 Acknowledgments

This work was supported by the Guangxi Natural Science Foundation under Grant No. 2022GXNSFBA035549.

References

[1] OGANESSIAN Y T, ABDULLIN F S, BAILEY P D, et al. Phys Rev Lett, 2010, 104: 142502. https://link.aps.org/doi/10.1103/PhysRevLett.104.142502.

[2] KHUYAGBAATAR J, YAKUSHEV A, DÜLLMANN C E, et al. Phys Rev Lett, 2014, 112: 172501. https://link.aps.org/doi/10.1103/PhysRevLett.112.172501.

[3] OGANESSIAN Y T, UTYONKOV V K, LOBANOV Y V, et al. Phys Rev C, 2006, 74: 044602. https://link.aps.org/doi/10.1103/PhysRevC.74.044602.

[4] OGANESSIAN Y T, UTYONKOV V K, LOBANOV Y V, et al. Phys Rev Lett, 1999, 83: 3154. https://link.aps.org/doi/10.1103/PhysRevLett.83.3154.

[5] OGANESSIAN Y T, UTYONKOV V K, LOBANOV Y V, et al. Phys Rev C, 2000, 62: 041604. https://link.aps.org/doi/10.1103/PhysRevC.62.041604.

[6] OGANESSIAN Y T, UTYONKOV V K, LOBANOV Y V, et al. Phys Rev C, 2004, 70: 064609. https://link.aps.org/doi/10.1103/PhysRevC.70.064609.

[7] UTYONKOV V K, BREWER N T, OGANESSIAN Y T, et al. Phys Rev C, 2015, 92: 034609. https://link.aps.org/doi/10.1103/PhysRevC.92.034609.

[8] ZAGREBAEV V, GREINER W. Phys Rev C, 2008, 78: 034610. https://link.aps.org/doi/10.1103/PhysRevC.78.034610.

[9] ZAGREBAEV V I. Phys Rev C, 2001, 64: 034606. https://link.aps.org/doi/10.1103/PhysRevC.64.034606.

[10] LIU Z H, BAO J D. Phys Rev C, 2009, 80: 054608. https://link.aps.org/doi/10.1103/PhysRevC.80.054608.

[11] ZHANG G, LI J J, ZHANG X R, et al. Phys Rev C, 2020, 102: 024617. https://link.aps.org/doi/10.1103/PhysRevC.102.024617.

[12] FENG Z Q. Phys Rev C, 2023, 107: 054613. https://link.aps.org/doi/10.1103/PhysRevC.107.054613.

[13] ZHU L, SU J, ZHANG F S. Phys Rev C, 2016, 93: 064610. https://link.aps.org/doi/10.1103/PhysRevC.93.064610.

[14] SEKIZAWA K, YABANA K. Phys Rev C, 2016, 93: 054616. https://link.aps.org/doi/10.1103/PhysRevC.93.054616.

[15] SUN X X, GUO L. Phys Rev C, 2023, 107: 064609. https://link.aps.org/doi/10.1103/PhysRevC.107.064609.

[16] TIAN J, WU X, ZHAO K, et al. Phys Rev C, 2008, 77: 064603. https://link.aps.org/doi/10.1103/PhysRevC.77.064603.

[17] LI C, ZHANG F, LI J, et al. Phys Rev C, 2016, 93: 014618. https://link.aps.org/doi/10.1103/PhysRevC.93.014618.

[18] FENG Z Q, JIN G M, LI J Q. Phys Rev C, 2009, 80: 057601. https://link.aps.org/doi/10.1103/PhysRevC.80.057601.

[19] FENG Z Q, JIN G M, FU F, et al. Nuclear Physics A, 2006, 771: 50. https://www.sciencedirect.com/science/article/pii/S0375947406001138. DOI: https://doi.org/10.1016/j.nuclphysa.2006.03.002.

[20] ZHU L, ZHANG F S, WEN P W, et al. Phys Rev C, 2017, 96: 024606. https://link.aps.org/doi/10.1103/PhysRevC.96.024606.

[21] ADAMIAN G G, ANTONENKO N V, SCHEID W. Phys Rev C, 2003, 68: 034601. https://link.aps.org/doi/10.1103/PhysRevC.68.034601.

[22] ZHANG G, LI J J, ZHANG X R, et al. Phys Rev C, 2020, 102: 024617. http://link.aps.org.https.yzn.proxy.chaoxing.com/doi/10.1103/PhysRevC.102.024617.

[23] WEISSKOPF V. Phys Rev, 1937, 52: 295. https://link.aps.org/doi/10.1103/PhysRev.52.295.

[24] JACKSON J D. Canadian Journal of Physics, 1956, 34(8): 767. https://doi.org/10.1139/p56-087.

[25] [EB/OL]. nrv.jinr.ru/nrv/.

[26] ZYROMSKI K E, LOVELAND W, SOULIOTIS G A, et al. Phys Rev C, 1997, 55: R562. https://link.aps.org/doi/10.1103/PhysRevC.55.R562.

[27] LÜ H, BOILLEY D, ABE Y, et al. Phys Rev C, 2016, 94: 034616. https://link.aps.org/doi/10.1103/PhysRevC.94.034616.

[28] ROUT P C, CHAKRABARTY D R, DATAR V M, et al. Phys Rev Lett, 2013, 110: 062501. https://link.aps.org/doi/10.1103/PhysRevLett.110.062501.

CNPC2023 探究在质子蒸发道中产生超重核的可行性

李路琦[1]，张 根[1]，蔡军军[1]，周立林[1]，张丰收[2, 3, 4]

(1. 广西大学物理科学与工程技术学院, 南宁 530004; ；
2. 北京师范大学核科学与技术学院，北京 100875；
3. 北京辐射中心，北京 100875；
4. 兰州重离子加速器国家实验室理论核物理中心，兰州 730000)

摘要：在双核系统（DNS）模型下系统地研究了质子蒸发道中产生超重核的可行性。由于 Z=114 质子壳层的存在，在质子蒸发道中合成 Fl 同位素是合适的。在本工作中我们只考虑了先蒸发一个质子，然后蒸发 n 个中子的情况，其他情况由于截面太小而被忽略。与 ^{50}Ti+^{243}Np 和 ^{54}Cr+^{239}Pa 反应相比，未知 ^{290,291}Fl 同位素在 ^{38}S+^{255}Es 反应中的产生截面最高，最大截面分别为 1.1 和 15.1 pb。未来随着放射性束设施的升级，^{42}S+^{254}Es 是接近稳定岛的一个有希望的弹靶体系，该反应中 $^{291-294}$Fl 的产生截面估计分别为 3.2、6.0、4.0 和 0.1 pb。

关键词：双核系统模型; 超重核素; 熔合反应; 质子蒸发道; 产生截面

收稿日期：2024-01-26；　**修改日期：**2024-01-26
基金项目：广西自然科学基金资助项目 (2022GXNSFBA035549)
通信作者：李路琦，E-mail: liluqi@st.gxu.edu.cn